Spectral analysis with short data batches (photon correlation spectroscopy)

1979 J. Phys. A: Math. Gen. 12 591

(http://iopscience.iop.org/0305-4470/12/4/018)

J. Phys. A: Math. Gen., Vol. 12, No. 4, 1979. Printed in Great Britain

Spectral analysis with short data batches

C J Oliver

Royal Signals and Radar Establishment, Malvern, Worcs, WR14 3PS, UK

Received 15 March 1978, in final form 17 August 1978

Abstract. This paper studies the limiting accuracy with which power spectra and the values of spectral parameters for random signals can be achieved from short batches of data. Initially, general expressions for arbitrary data are derived; these are then restricted for simplicity to wide-band signals. In addition, comparison is made with computer simulation for two well defined models, namely, photodetection of light of constant intensity and heterodyne photodetection of narrow-band Gaussian–Lorentzian light. It is shown that there is no analytical difference between operation in time or frequency space for batch data, and also that long data sets can be analysed at least as well, in terms of the accuracy with which spectral parameters can be determined by fitting, by averaging over many short batches as by processing the set as a whole.

1. Introduction

In this paper we shall be concerned with the estimation of the spectral properties of random signals from truncated sets of data. For random signals the most meaningful spectral estimators are the autocorrelation function (time space) and its Fourier transform pair, the power spectrum (frequency space). The fact that only a finite record of the signal is available for spectral analysis results in a discrepancy between the observed spectral estimator and its true, infinite-duration, value. Much effort has been concentrated in the past on the choice of suitable window functions to attempt to 'restore' the true spectral shape by reducing side lobes, etc. Of course these techniques, while they may give a better appearance to the observed spectral estimator, have actually introduced correlations in the data corresponding to the impulse function of the spectral weighting filter adopted. Where spectra are sufficiently complicated it is often useful to obtain such a display, in spite of its shortcomings, since it enables one to study the features of the spectrum. However, there are many applications where the spectrum is essentially very simple and can be characterised by a suitable model. In these cases there is no advantage, indeed the reverse, in weighting the original data. The best results will be obtained by fitting the observed spectral estimators to the theoretical form corresponding to the model of the process with truncation effects included. In this type of analysis one is not basically concerned with the form of the spectral estimator *per se*, but with extracting a few simple parameters, such as peak position and linewidth, which give information about the process under study. This type of analysis forms the basis of nearly all photon-correlation spectroscopy of optical signals, for example. This paper will concentrate on this latter type of spectral analysis and will indeed be applied specifically as an example to the extraction of spectral properties in photon-correlation spectroscopy. It differs, therefore, in three respects from previous papers dealing

0305-4470/79/040591+27$01.00

specifically with the accuracy with which spectral parameters can be determined in photon-correlation spectroscopy (Jakeman *et al* 1970, 1971b, Degiorgio and Lastovka 1971, Kelly 1971, Saleh and Cardoso 1973, Hughes *et al* 1973, Jakeman 1972, 1974, Oliver 1974, 1978; the last three references in particular serve as reviews of the field). Firstly, general results are presented which are subsequently applied to the specific case of photon-correlation spectroscopy as an example. Secondly, a comparison of spectral analysis in time and frequency spaces is given rather than analysis merely in time space. Thirdly, the effect of analysing short batches of data is considered and subsequently compared with the use of long data sets as described previously.

It is important to compare the errors that are obtained in the spectral estimators and fitted parameters when operating in either delay-time or frequency space, since instrumentation is available with acceptable performance in both domains. In time space the autocorrelator, particularly in its digital implementation (Foord *et al* 1969, 1970) enables parallel-channel, real-time processing at bandwidths up to about 10 MHz. In frequency space the discrete Fourier transform (DFT) could now be performed at similar speeds on dedicated computers; alternatively an implementation of the chirp Z transform (CZT) using acoustic surface wave technology (Butler 1977) offers comparable bandwidth with analog signals. Another possibility in frequency space is the bank of filters. All these instruments are parallel-channel devices in that many frequency or time-delay components are processed simultaneously. For the sake of comparison we shall also assume that one can actually implement ideal processing with no dynamic range, bandwidth or linearity restrictions in either domain.

Sections 2–5 of this paper concentrate on the extraction of the maximum amount of information from a set of N real, discrete data points $(x(0) \ldots x(N-1))$. Operation in both frequency and time spaces is considered. Section 6 addresses the comparison of the performance that can be achieved by averaging over many (M/N) short batches of length N with that obtained by continuous processing with a long data set of duration $M(\gg N)$ samples. The digital autocorrelator and the filter bank are generally operated in this latter mode, whereas the DFT and the CZT (and, in some applications, the autocorrelator) are essentially batch processors of the former type.

Let us now discuss the different spectral analysis methods that can be applied to a batch of data of length N. From the initial data (A) one can proceed either in delay-time space by constructing an estimate of the autocorrelation function (B) or one can construct the periodogram by taking the square of the modulus of the DFT of the signal data (D). From the autocorrelation function estimate (B) one could transfer from time to frequency space by taking the Fourier transform to obtain a power spectrum estimator (C). In § 2 we will compare different power spectrum estimators obtained by the route ABC with the periodogram obtained by the route AD for any set of data $x(0)$ to $x(N-1)$. Having chosen suitable spectral estimators in time and frequency space we next derive their means and variances in § 3.1. For simplicity we consider only wide-band signals such that the data in neighbouring samples are uncorrelated. These results are then compared with simulation for the specific case of heterodyne photodetection of Gaussian–Lorentzian light in § 3.2. This situation is well understood both theoretically and experimentally (Jakeman *et al* 1971a). In addition a full analysis, including the simulation technique, for long data sets has been described in detail in Oliver (1978).

After comparing the properties of the different spectral estimators (B, C and D) in § 3 we next go on to consider the extraction of spectral parameters by fitting the estimators to the model which describes the process. Simulation and theory for

autocorrelation function analysis have previously been compared in some detail for long data sets with the same optical heterodyne detection conditions (Oliver 1978). In the present paper we shall be comparing the results of simulation as different spectral estimators are employed; detailed theoretical comparison is not attempted. Before attempting to fit the estimators one must first consider whether it is possible to normalise the data so as to reduce the relative fluctuations in the spectral estimator coefficients. This has been discussed previously for photodetection in Jakeman *et al* (1970, 1971b), Hughes *et al* (1973), Koppel (1974) and Oliver (1974, 1978). Here we consider first wide-band signals of arbitrary statistics before making detailed comparison for the special case of photodetection of a constant light intensity. Normalisation of the autocorrelation function is considered in § 4.1 with the means and variances derived in § 4.1.1 and compared with simulation in § 4.1.2. The equivalent treatment for the periodogram is given in § 4.2. The properties of the spectral estimators are then summarised in § 4.3.

In many situations one is not concerned primarily with the spectrum itself but with particular information contained in the spectrum, such as peak positions and widths. In cases where the process giving rise to the spectrum is well understood we have a model which can be used to fit the spectrum to obtain values of specific spectral parameters. For heterodyne photodetection of Gaussian–Lorentzian light we have taken a two-parameter model based on a frequency shift ω_0 and linewidth Γ. Thus the final step in extracting these parameters is to perform a least-squares fitting procedure on the spectral estimates. One then arrives at estimates for ω_0 and Γ via the three different routes AB, ABC, AD. The final comparison for short data batches, made using simulation as before, is of the relative accuracy of these parrameters determined through the different analysis methods as described in § 5.

Having compared the use of frequency and time domains in spectral analysis in §§ 2–5 we next (§ 6) go on to consider the situation where the data are available as a long string of samples $M (M \gg N)$. Those processing options which use batch processing will take a batch of data of lengths N (A) and construct either the autocorrelation function estimator (B) or the periodogram (C). These estimators can then be normalised, summed and averaged over M/N batches giving new spectral estimators D and E respectively. Continuous-operation devices take the long data set (A′) and construct, for example, the autocorrelation function estimator for N delay coefficients (F). Finally these three spectral estimators can be fitted to the specific model, and the relative accuracy of the spectral parameters by the three routes (ABD, ACE, A′F) compared.

In this paper, therefore, we proceed on three levels. Firstly there are completely general results for all types of signal; secondly there are results which apply specifically to wide-band signals; and thirdly there are results which relate to the particular model chosen for comparison purposes.

2. Spectral estimators

As we have seen, one method of describing the spectral properties of a random signal is via its autocorrelation function. Following equation (11.19) of Oppenheim and Schafer (1975), this may be defined as

$$R(k) = \frac{1}{N} \sum_{j=0}^{N-1-|k|} x(j) x^*(j+k). \tag{1}$$

For real data $x^* = x$ and the function is symmetric about $k = 0$ with $|k| \leq N-1$. If we wish to transfer to frequency space, the discrete Fourier transform of the autocorrelation function is given by

$$S^{(1)}(\omega) = \sum_{k=-N+1}^{N-1} R(k) \exp(-i\Omega k) = \frac{2}{N} \sum_{k=0}^{N-1} \sum_{j=0}^{N-1-k} x(j)x(j+k) \cos(\Omega k) - \frac{1}{N} \sum_{j=0}^{N-1} x^2(j) \tag{2}$$

where $\Omega = \omega T$, ω being the angular frequency and T the separation of the samples.

Alternatively one may proceed directly into frequency space. For a continuous function $x(t)$, the power spectrum can be defined by

$$S(\omega) = \lim_{\mathcal{T} \to \infty} \frac{1}{\mathcal{T}} \left| \int_{-\mathcal{T}/2}^{+\mathcal{T}/2} x(t) \exp(-i\omega t)\, dt \right|^2 \tag{3}$$

where $\mathcal{T}$ is the duration of the data. For a batch of N discrete samples of the real variable $x(j)$, where j refers to a particular sample, an equivalent power spectral estimator could be defined by

$$P(\omega) = \frac{1}{N} \left| \sum_{j=0}^{N-1} x(j) \exp(-i\Omega j) \right|^2. \tag{4}$$

When $\omega = 2\pi l/NT$ this estimator is known as the 'periodogram' of the data as shown in equation (11.25) of Oppenheim and Schafer (1975). Expanding equation (4) and rearranging we obtain

$$P\left(\frac{2\pi l}{NT}\right) = \frac{2}{N} \sum_{k=0}^{N-1} \sum_{j=0}^{N-1-k} x(j)x(j+k) \cos\left(\frac{2\pi lk}{N}\right) - \frac{1}{N} \sum_{j=0}^{N-1} x^2(j). \tag{5}$$

The equivalence of the spectral estimator $S^{(1)}(\omega)$, obtained from the autocorrelation function as in equation (2), with the periodogram defined in equations (4) and (5) is the form of the Wiener–Khinchin relation for finite sets of discrete samples of a random ergodic signal.

Thus the two spectral estimators in frequency space, obtained by routes ABC and AD, are identical when these particular definitions are adopted. Since the final accuracy with which the spectral parameters can be obtained through fitting C and D must be identical, one would also expect fitting the autocorrelation function, B, to give the same accuracy, except for differences in the weighting applied to the parameters when fitting in the two spaces. This would imply that one's choice of method should be determined only by engineering considerations, since there is no appreciable theoretical difference.

On proceeding via the autocorrelation function, the power spectrum estimator $S^{(1)}(\omega)$ is not the only reasonable one to adopt. Since the autocorrelation function is reflected about zero delay, one can ignore negative values of k and the imaginary term in the Fourier transform. The resultant power spectrum estimator will then be given by

$$S^{(2)}\left(\frac{2\pi l}{NT}\right) = \frac{1}{N} \sum_{k=0}^{N-1} \sum_{j=0}^{N-1-k} x(j)x(j+k) \cos\left(\frac{2\pi lk}{N}\right) = \frac{1}{2} P\left(\frac{2\pi l}{NT}\right) + \frac{1}{2N} \sum_{j=0}^{N-1} x^2(j). \tag{6}$$

This estimator is equal to half the periodogram plus a flat background term corresponding to the estimator for the mean-square value of the data. This background term is also encountered if the original value of the autocorrelation function at zero delay is

unknown and taken to be zero in the Fourier transform. In this case equation (5) would be modified so that

$$S_N^{(3)}(\omega) = P(\omega) - \frac{1}{N}\sum_{j=0}^{N-1} x^2(j) \tag{7}$$

where $\omega = 2\pi l/NT$, while equation (6) would become

$$S^{(4)}(\omega) = \tfrac{1}{2}P(\omega) - \frac{1}{2N}\sum_{j=0}^{N-1} x^2(j). \tag{8}$$

For each of the spectral estimators $S^{(2)}(\omega)$, $S^{(3)}(\omega)$ and $S^{(4)}(\omega)$, one has the same spectral shape as the periodogram but with different, though related, flat background contributions. If the estimator for the mean-square value of the data is independently measured, this background introduces no problem. However, if it is unknown, one has either to include a further variable in any least-squares fitting routine, which reduces the accuracy with which the parameters can be obtained, or to find some other method of removing the background, as will be discussed in § 4.2.

A fifth type of power spectrum estimator which could be derived from the autocorrelation function would be to reflect the autocorrelation function about the zero delay and then take the full complex Fourier transfor, i.e. ignoring the known phase of the autocorrelation function. In this case the spectral estimator would be defined similarly to equation (5) above, giving

$$S^{(5)}(\omega) = \frac{2}{N}\sum_{k=0}^{N-1}\sum_{j=0}^{N-1} R(j)R(j+k)\cos\left(\frac{2\pi lk}{N}\right) - \frac{1}{N}\sum_{j=0}^{N-1}(R(j))^2. \tag{9}$$

Expanding in terms of the original data we obtain

$$S^{(5)}(\omega) = \frac{2}{N^3}\sum_{k=0}^{N-1}\sum_{j=0}^{N-1-k}\sum_{s=0}^{N-1-j}\sum_{r=0}^{N-1-j-k} x(s)x(s+j)x(r)x(r+j+k)\cos\left(\frac{2\pi lk}{N}\right)$$
$$-\frac{1}{N^3}\sum_{j=0}^{N-1}\sum_{s=0}^{N-1-j} x^2(s)x^2(s+j) \tag{10}$$

which, in turn, as in equation (4), is also equal to

$$S^{(5)}(\omega) = \frac{1}{N}\left|\frac{1}{N}\sum_{k=0}^{N-1}\sum_{j=0}^{N-1-k} x(j)x(j+k)\exp\left(-\frac{\mathrm{i}2\pi lk}{N}\right)\right|^2. \tag{11}$$

This spectral estimator contains terms in the fourth power of the data which are of the wrong dimensions for a power spectrum. Also its detailed form is not simply related to any previous estimator. The dimensions could be corrected by taking the square root of this estimator, though the shape will still not correspond to the periodogram. While this last estimator may not be suitable as a means of representing the power spectrum or, in particular, when used to measure linewidth, this does not preclude its usefulness as a means of determining the mean frequency. It may even offer advantages in this respect, as has been demonstrated in simulation work for photodetection of a sinusoidal intensity (Pike 1977). The author compared the periodogram of a set of data (his figure 16) with the complex Fourier transform of the autocorrelation function followed by taking the square of the modulus as in equation (11) above (his figure 6). This latter is a noticeably smoother spectral estimator which enabled the mean frequency to be determined with smaller statistical fluctuations. However, the shape at low frequencies

is significantly different from that of the periodogram. This result may indicate that one should choose one's spectral estimator in such a way as to minimise the errors in the particular parameter of interest; this will obviously differ from case to case.

3. Properties of the spectral estimator

Having chosen a consistent pair of spectral estimators, which we shall take as defined by equation (1) for the autocorrelation function and by equation (4) for the power spectrum (the periodogram), we next investigate their properties. It is necessary to establish whether there is any *bias* in each estimator, i.e. the extent to which the ensemble average of the estimator differs from its true value, and also to determine whether the estimators are *consistent*, i.e. whether the variance tends to zero as the number of samples increases without limit. We require, therefore, to derive the mean and variance of the spectral estimators. Initially we shall derive expressions for these quantities for arbitrary signal $x(j)$. Subsequently this will be simplified to consider wide-band signals. In order to make comparison with simulation we shall take two specific cases. Firstly we shall consider photodetection of a constant-intensity light source, which allows detailed comparison. Secondly we shall consider heterodyne photodetection of narrow-band Gaussian–Lorentzian light. Here we shall use the exact theory for the mean values of the estimators, but only the theory for the weak-signal limit for the variances.

3.1. Theoretical predictions

Derivation of the mean and variance of the autocorrelation function has already been described for the case when the total number of samples is much greater than the number of delay coefficients calculated, i.e. $N \gg k$ (Jakeman *et al* 1970, 1971b, Oliver 1978). With short data batches, however, we are in the region $N \sim k$, so that end effects, which could be ignored in the previous work, dominate.

Provided that the variable x is stationary and ergodic, the ensemble average of the autocorrelation function estimator defined in equation (1) is given by

$$\langle \hat{R}(k) \rangle = [(N - |k|)/N] R(k) \tag{12}$$

where the presence of a 'hat' denotes an estimator, and its absence the true value. This estimator is biased by an amount proportional to k/N. A related definition of the autocorrelation function estimator which would remove this bias would be (equation (11.17) of Oppenheim and Schafer)

$$\hat{R}(k) = \frac{1}{N - |k|} \sum_{j=0}^{N-1-|k|} x(j) x^*(j+k). \tag{13}$$

However, taking the DFT of this autocorrelation function estimator would not yield the periodogram. Therefore, if we wish to perform analysis in time space, it may be advantageous to use the unbiased estimator for the autocorrelation function defined in equation (13). If, however, we wish to proceed via the autocorrelation function to the periodogram, the definition of equation (1) should be retained. Of course, in the limit as N tends to infinity but k remains small, both estimators are equivalent, since equation (12) shows that the original estimator chosen is asymptotically unbiased.

Adopting the second definition of the autocorrelation function estimator, the ensemble average is given by

$$\langle \hat{R}(k) \rangle = \frac{1}{N-k} \sum_{j=0}^{N-1-k} \langle x(j)x(j+k) \rangle = R(k) \tag{14}$$

since

$$\sum_{j=0}^{N-1-k} 1 = N-k$$

as desired, and the mean-square value is given by

$$\langle \hat{R}^2(k) \rangle = \frac{1}{(N-k)^2} \sum_{j=0}^{N-1-k} \sum_{l=0}^{N-1-k} \langle x(j)x(j+k)x(l)x(l+k) \rangle. \tag{15}$$

If we separate out the special cases $l=j$, $l=j+k$, $l=j-k$ we obtain

$$\langle \hat{R}^2(k) \rangle = \frac{1}{(N-k)^2} \left(\sum_{j=0}^{N-1-k} \langle x^2(j)x^2(j+k) \rangle + 2 \sum_{j=0}^{N-1-2k} \langle x(j)x^2(j+k)x(j+2k) \rangle \right.$$
$$\left. + \sum_{j=0}^{N-1-k} \sum_{\substack{l \neq j \\ \neq j+k \\ \neq j-k \\ =0}}^{N-1-k} \langle x(j)x(j+k)x(l)x(l+k) \rangle \right) \tag{16}$$

for $k \leqslant (N-1)/2$. In the last term of equation (16) there is a further limitation on the choice of l and j such that $l+j \leqslant 2(N-1-k)$, so that j and l both lie within the required bounds simultaneously. For $k \geqslant N/2$ one obtains the simpler expression

$$\langle \hat{R}^2(k) \rangle = \frac{1}{(N-k)^2} \left(\sum_{j=0}^{N-1-k} \langle x^2(j)x^2(j+k) \rangle + \sum_{j=0}^{N-1-k} \sum_{\substack{l \neq j \\ =0}}^{N-1-k} \langle x(j)x(j+k)x(l)x(l+k) \rangle \right). \tag{17}$$

Combining equations (14) with (16) or (17) the variance can be calculated. This will depend on the detailed properties of x which determine any factorisation that can be applied.

If we next make the equivalent derivation for the periodogram, as defined in equation (4), the mean value will be given by

$$\langle \hat{P}(\omega) \rangle = \frac{1}{N} \sum_{j=0}^{N-1} \sum_{k=0}^{N-1} \langle x(j)x(k) \rangle \exp[-i\Omega(j-k)] \tag{18}$$

which is unbiased, where $\omega = (2\pi/NT) \times$ integer and $\Omega = \omega T$. Separating into diagonal and off-diagonal terms this becomes

$$\langle \hat{P}(\omega) \rangle = \langle x^2 \rangle + \frac{1}{N} \sum_{j=0}^{N-1} \sum_{\substack{k \neq j \\ =0}}^{N-1} \langle x(j)x(k) \rangle \exp[-i\Omega(j-k)]. \tag{19}$$

Similarly the mean-square value is given by

$$\langle \hat{P}^2(\omega) \rangle = \frac{1}{N^2} \sum_{\substack{j,k,l,m \\ =0}}^{N-1} \langle x(j)x(k)x(l)x(m) \rangle \exp[-i\Omega(j-k+l-m)]. \tag{20}$$

Separating out the special cases as before when two or more samples are identical, we obtain

$$\langle \hat{P}^2(\omega)\rangle = \frac{1}{N^2}\Bigg(\sum_{j=0}^{N-1}\langle x^4(j)\rangle + \sum_{j=0}^{N-1}\sum_{\substack{k\neq j\\=0}}^{N-1}\{4\langle x^3(j)x(k)\rangle \exp[-i\Omega(j-k)]$$

$$+2\langle x^2(j)x^2(k)\rangle + \langle x^2(j)x^2(k)\rangle \exp[-i\Omega(2j-2k)]\}$$

$$+\sum_{j=0}^{N-1}\sum_{\substack{k\neq j\\=0}}^{N-1}\sum_{\substack{l\neq k\\\neq j\\=0}}^{N-1}\{4\langle x^2(j)x(k)x(l)\rangle \exp[-i\Omega(k-l)]$$

$$+2\langle x^2(j)x(k)x(l)\rangle \exp[-i\Omega(2j-k-l)]\}$$

$$+\sum_{j=0}^{N-1}\sum_{\substack{k\neq j\\=0}}^{N-1}\sum_{\substack{l\neq k\\\neq j\\=0}}^{N-1}\sum_{\substack{m\neq l\\\neq k\\\neq j\\=0}}^{N-1}\langle x(j)x(k)x(l)x(m)\rangle \exp[-i\Omega(j-k+l-m)]\Bigg). \tag{21}$$

Hence the variance can be evaluated which will depend on the properties of x. Let us now consider the three specific cases mentioned previously.

3.1.1. Wide-band signals. For wide-band signals the data in different sample times are uncorrelated so that the x's will factorise. Thus equations (14), (16) and (17) for the mean and mean-square values of the autocorrelation function estimator will yield

$$\langle \hat{R}(k)\rangle = \langle x\rangle^2 \tag{22}$$

for the mean value and

$$\text{var}\,\hat{R}(k) = (\langle x^2\rangle^2 - \langle x\rangle^4)/(N-k) \tag{23}$$

when $k \geqslant N/2$ with an additional term

$$+[2(N-2k)/(N-k)^2]\langle x\rangle^2 \,\text{var}\, x$$

when $k \leqslant (N-1)/2$ for the variance. This derivation uses the properties that

$$\sum_{j=0}^{N-1-k}\sum_{\substack{l\neq j\\=0}}^{N-1-k} 1 = (N-k)(N-k-1), \qquad l+j \leqslant 2(N-1-k)$$

and

$$\sum_{j=0}^{N-1-k}\sum_{\substack{l\neq j\\\neq j+k\\\neq j-k\\=0}}^{N-1-k} 1 = \sum_{j=0}^{N-1-k}\sum_{l=0}^{N-1-k} 1 - \sum_{j=0}^{N-1-k} 1 - 2\sum_{j=0}^{N-1-2k},$$

$$= (N-k)^2 - (N-k) - 2(N-2k).$$

From equations (22) and (23) it is apparent that, for wide-band signals, the autocorrelation function estimator is both unbiased and consistent. In general, when it is not possible to factorise the terms in equations (16) and (17) as was done here, there will be terms of order unity remaining in the expression for the variance in addition to those of order $1/(N-k)$ given here. Under these conditions, when the signal in

neighbouring samples is correlated, the autocorrelation function estimator will not be consistent, therefore.

Making the same factorisation in equations (19) and (21) we find that the mean and variance of the periodogram are given by

$$\langle \hat{P}(\omega) \rangle = \langle x^2 \rangle - \langle x^2 \rangle = \text{var } x \tag{24}$$

and

$$\text{var } \hat{P}(\omega) = (\text{var } x)^2 + N^{-1}(\langle x^4 \rangle - 4\langle x \rangle \langle x^3 \rangle - 3\langle x^2 \rangle^2 + 12\langle x \rangle^2 \langle x^2 \rangle - 6\langle x \rangle^4) \tag{25}$$

since

$$\sum_{j=0}^{N-1} \sum_{\substack{k=0 \\ k \neq j}}^{N-1} \exp[-i\Omega(j-k)] = -N, \quad \sum_{j=0}^{N-1} \sum_{\substack{k=0 \\ k \neq j}}^{N-1} \sum_{\substack{l=0 \\ l \neq k \\ l \neq j}}^{N-1} 1 = N^3 - 3N^2 + 2N$$

$$\sum_{j=0}^{N-1} \sum_{\substack{k=0 \\ k \neq j}}^{N-1} \sum_{\substack{l=0 \\ l \neq k \\ l \neq j}}^{N-1} \exp[-i\Omega(k-l)] = -N^2 + 2N, \quad \sum_{j=0}^{N-1} \sum_{\substack{k=0 \\ k \neq j}}^{N-1} \sum_{\substack{l=0 \\ l \neq k \\ l \neq j}}^{N-1} \exp[-i\Omega(2j-k-l)] = 2N$$

and

$$\sum_{j=0}^{N-1} \sum_{\substack{k=0 \\ k \neq j}}^{N-1} \sum_{\substack{l=0 \\ l \neq k \\ l \neq j}}^{N-1} \sum_{\substack{m=0 \\ m \neq l \\ m \neq k \\ m \neq j}}^{N-1} \exp[-i\Omega(j-k+l-m)] = 2N^2 - 6N.$$

Thus the periodogram is unbiased but is not a consistent estimator for the power spectrum even for wide-band signals, since the dominant term in the variance is independent of N. However, this does not imply that there is any difference in the spectral information contained in the periodogram (which is not consistent) and the autocorrelation function estimator (which is consistent) since the estimators are related by a linear process (the Fourier transform).

A similar result to equation (25) for wide-band random signals has been given by Hannan (1960) and Brillinger and Rosenblatt (1967). If, in addition, the probability distribution of x is Gaussian, i.e. white Gaussian noise, then the term in order $1/N$ reduces to zero (Oppenheim and Schafer 1975). In general it will not be possible to make the factorisation used in deriving the expressions for both mean and variance given in equations (24) and (25). Jenkins and Watts (1968) considered non-white Gaussian signals, i.e. when the probability distribution of x is Gaussian but the values of x are correlated. The mean value of the periodogram is no longer equal to the variance of the data, and the dominant term in the variance was shown to be given by

$$\text{var } \hat{P}(\omega) = <\hat{P}(\omega)>^2. \tag{26}$$

This is a more general case than white Gaussian noise, which it includes as a special case since equation (24) would then hold.

3.1.2. Photodetection of constant intensity. If we wish to make comparison between theory and simulation for the specific case of photodetection of a constant-intensity light source, the variable x now corresponds to the number of photodetections n occurring during the sample of duration T. For a constant intensity these properties are well known, the probability distribution of n being Poissonian (Mandel 1959). Since

the number of photodetections in each sample time is independent, the expressions for wide-band signals also apply to this case. Hence, for the autocorrelation function estimator,

$$\langle \hat{R}(k) \rangle = \langle n \rangle^2 \tag{27}$$

and

$$\text{var } \hat{R}(k) = \langle n \rangle^2 (1 + 2\langle n \rangle)/(N-k) \tag{28}$$

when $k \geq N/2$. For $k \leq (N-1)/2$ equation (28) contains the additional term

$$+[2(N-2k)/(N-k)^2]\langle n \rangle^3.$$

Similarly for the periodogram

$$\langle \hat{P}(\omega) \rangle = \langle n \rangle \tag{29}$$

and

$$\text{var } \hat{P}(\omega) = \langle n \rangle^2 + \langle n \rangle / N. \tag{30}$$

3.1.3. Heterodyne photodetection of narrow-band Gaussian–Lorentzian light. As has already been indicated, analytic derivation of the variance of the spectral estimators when the data in neighbouring samples are correlated is too cumbersome to be worthwhile. In this section, therefore, we shall derive *exact* expressions for the mean values of the spectral estimators, but only *approximate* values for the variances.

The true autocorrelation function for photodetection will be given by

$$R(k) = \langle n(0) n(k) \rangle$$

for stationary, ergodic signals. For heterodyne detection of Gaussian–Lorentzian light this yields

$$R(k) = (\bar{n}_o + \bar{n}_s)^2 + 2\bar{n}_o \bar{n}_s \cos(\omega_0 kT) \exp(-|\Gamma kT|) + \bar{n}_s^2 \times \exp(-|2\Gamma kT|) + (\bar{n}_o + \bar{n}_s)\delta_{k,0} \tag{31}$$

where Γ is the linewidth, ω_0 is the frequency shift, and we have replaced ensemble averages $\langle n \rangle$ with time averages $\bar{n}$ so that the mean signal and local oscillator counts per sample time are given by $\bar{n}_s$ and $\bar{n}_o$ respectively. The normalised version of the intensity correlation function for heterodyne detection was previously given by Jakeman (1972, 1974). The autocorrelation function estimator in equation (13) has this mean value. In order to derive the variance of this estimator we shall follow Jakeman (1972) in assuming that we are in the weak-signal limit ($\bar{n}_s \ll 1$), so that the statistical fluctuations are dominated by the shot noise in the local oscillator. The number of photodetections in neighbouring samples is then essentially uncorrelated so that the wide-band theory is again applicable. The variance is then as given in equation (28) with $\langle n \rangle$ replaced by $\bar{n}_o$.

From equations (2) and (5) the periodogram can be derived by taking the DFT of the autocorrelation function in equation (1), which is related to $R(k)$ as shown in equation (12). Substituting into equation (5), therefore, the mean value of the periodogram for heterodyne photodetection of narrow-band Gaussian–Lorentzian light can be shown to be given by

$$\langle P(\omega) \rangle = \frac{2}{N} \sum_{k=0}^{N-1} (N-k)[(\bar{n}_o + \bar{n}_s)^2 + 2\bar{n}_o \bar{n}_s \cos(\omega_0 kT) \exp(-\Gamma kT) + \bar{n}_s^2 \exp(-2\Gamma kT) + (\bar{n}_o + \bar{n}_s)\delta_{k,0}] \cos(\omega kT) - R(0). \tag{32}$$

Performing the transformation one obtains

$$\langle P(\omega)\rangle = 2\bar{n}_o\bar{n}_s\left(\frac{1-e^{-\gamma}\cos\Omega_s}{1-2e^{-\gamma}\cos\Omega_s+e^{-2\gamma}}+\frac{1-e^{-\gamma}\cos\Omega_d}{1-2e^{-\gamma}\cos\Omega_d+e^{-2\gamma}}\right)+\bar{n}_o(1-2\bar{n}_s)$$
$$+2\bar{n}_s^2\frac{1-e^{-2\gamma}\cos\Omega}{1-2e^{-2\gamma}\cos\Omega+e^{-4\gamma}}+\bar{n}_s(1-\bar{n}_s)+(\bar{n}_o+\bar{n}_s)^2N\delta(\omega)$$
$$-\frac{1}{N}\left[2\bar{n}_o\bar{n}_s\,e^{-\gamma}\left(\frac{e^{-2\gamma}\cos\Omega_s-2e^{-\gamma}+\cos\Omega_s}{(e^{-2\gamma}-2e^{-\gamma}\cos\Omega_s+1)^2}+\frac{e^{-2\gamma}\cos\Omega_d-2e^{-\gamma}+\cos\Omega_d}{(e^{-2\gamma}-2e^{-\gamma}\cos\Omega_d+1)^2}\right.\right.$$
$$\left.\left.-2\bar{n}_s^2\,e^{-2\gamma}\frac{e^{-4\gamma}\cos\Omega-2e^{-2\gamma}+\cos\Omega}{(e^{-4\gamma}-2e^{-2\gamma}\cos\Omega+1)^2}\right]\right. \tag{33}$$

where $\Omega=\omega T$, $\Omega_s=(\omega+\omega_0)T$, $\Omega_d=(\omega-\omega_0)T$ and $\gamma=\Gamma T$. The variance of the periodogram, using the same simplifying assumption as before, is then obtained by substituting $\bar{n}_o$ for $\langle n\rangle$ in equation (30).

3.2. Comparison of simulation with theory

Having derived the relevant theoretical expressions for the means and variances of the spectral estimators for the two specific cases of photodetection of constant intensity and heterodyne photodetection of narrow-band Gaussian–Lorentzian light, let us now compare these results with simulation. The simulation method was first described in Hughes *et al* (1973), where it was applied to direct detection. In Oliver (1978) it was then extended to cover heterodyne detection, which is the form in which it will be used in the present paper.

Initially let us make a comparison of the results for constant intensity. These results are summarised in table 1. The simulation was performed for 1000 batches each of duration $N = 128$ and with a mean photodetection count rate per sample time of $\bar{n} = 10$. Equations (23) and (28) indicated that the variance of the autocorrelation function estimator should be a function of k. Accordingly simulation and theory are compared for three distinct values of k (1, 63 and 127). Over the complete range the comparison shows close agreement between theory and simulation, both for the mean value and for the variance. The dramatic increase in the error in the autocorrelation function estimator for large delays implies that there is little to be gained in seeking to extract spectral information from the longest delay channels. In practice the first 70% of the

Table 1. A comparison of the theoretical predictions for the autocorrelation function and periodogram estimators with simulation over 1000 sequences with a constant mean photodetection count rate of $\bar{n} = 10$.

Estimator	Component	Mean		Variance	
		Simulation	Theory	Simulation	Theory
Autocorrelation function	1	99·91	100	33·8	32·1
	63	99·92	100	35·2	33·3
	127	98·90	100	1982	2100
Periodogram	Average over 1 to 64	9·99 ± 0·04	10	100·2 ± 1·2	100·1

autocorrelation function has similar accuracy, but beyond this point the error increases rapidly. For the periodogram equations (25) and (30) indicated that the variance should be independent of frequency, while equations (24) and (27) show the same for the mean value. The periodogram, therefore, which has 64 coefficients, is compared by averaging all frequency components of the simulated data. Again the agreement between theory and simulation is within the statistical accuracy. Since the variance is independent of delay, one should use all the coefficients when determining spectral parameters by fitting the periodogram.

Following this comparison for constant intensity we next make a similar comparison for heterodyne detection of Gaussian–Lorentzian light. Simulation over 100 batches each of length $N = 128$ was performed with $\bar{n}_o = 10$ and $\bar{n}_s = 0{\cdot}2$. The period ($\tau_p = 2\pi/\omega_0$) was selected to be 10·24 sample times (T), and the coherence time ($\tau_c = 1/\Gamma$) 10 sample times. The comparison of the simulated mean value and standard deviation with theory for the autocorrelation function estimator, shown in figure 1, demonstrates qualitative agreement throughout. Since the signal is only weak ($n_s < 1$), one would expect the simple theory for the variance to be reasonable, as is the case. The estimate of the mean value of the autocorrelation function after 100 batches have been averaged shows a discrepancy which is caused by the statistical fluctuations in the total number of photodetections per batch in simulated data. This apparent misnormalisation was the justification for introducing different methods of normalising the autocorrelation function as discussed in Oliver (1978). This aspect will be treated more deeply later.

A similar comparison, this time for the periodogram, based on the identical data is shown in figure 2. For convenience the vertical scale of the standard deviation has been displaced with respect to the mean value. The agreement between the exact theory for the mean value (equation (33)) and simulation is good. Moreover, it should be noted that the predicted value of the periodogram away from the peak in the weak-signal limit might be expected to be 10·0 from equation (24), whereas the simulated value lies

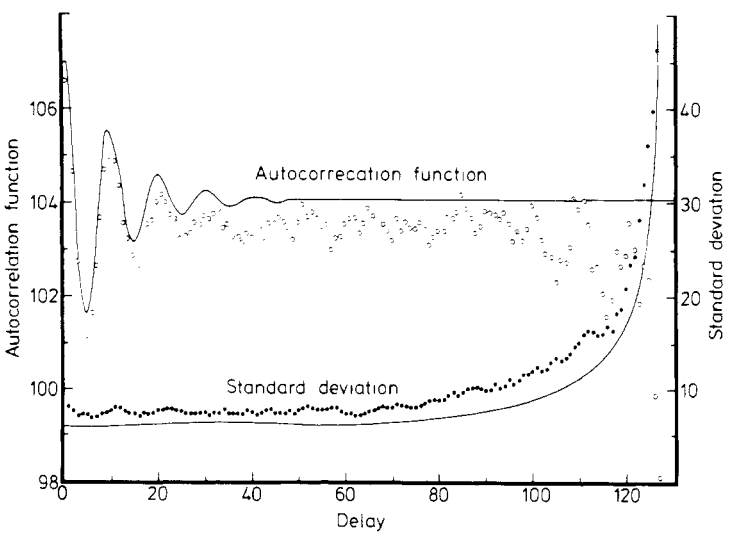

Figure 1. A comparison of the simulated and theoretical values of the mean and standard deviation of the autocorrelation function estimator for heterodyne photodetection of narrow-band Gaussian–Lorentzian light. The full curves represent theory. Simulation conditions: 100 batches, $N = 128$, $\bar{n}_o = 10$, $\bar{n}_s = 0{\cdot}2$, $\tau_p/T = 10{\cdot}24$, $\tau_c/T = 10$.

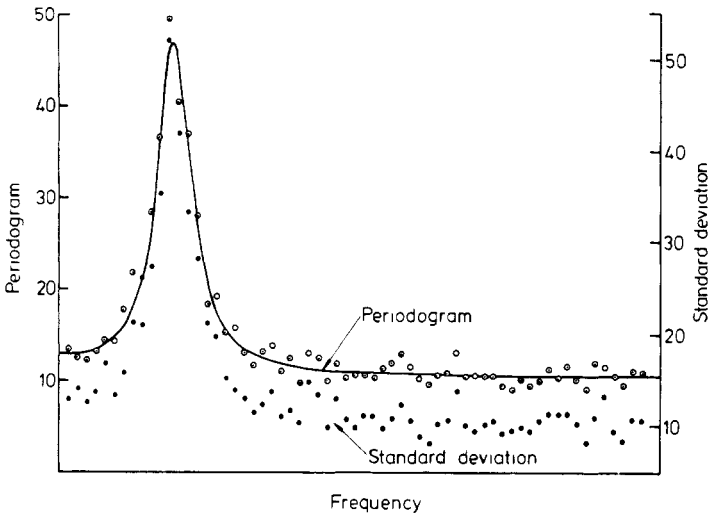

Figure 2. A comparison of the simulated and theoretical values of the mean of the periodogram under the same conditions as in figure 1. The simulated results for the standard deviation are displaced with respect to the mean value.

around the exact theoretical value of 10·5. Similarly the expected standard deviation away from the peak would be expected to be about 10·004 from equation (30), which is again consistent with simulation. However, comparison of the standard deviation with the mean value for the averaged periodograms of the simulated data over the whole spectral range shows that equation (26), which was derived for a Gaussian distribution of x, also applies to photodetection of light with a Gaussian optical field amplitude distribution, even though $p(n)$ is not Gaussian. In fact for large oscillator power ($\bar{n}_o \gg \bar{n}_s$, $\bar{n}_o \gg 1$) the distribution $p(n)$ does tend towards a Gaussian distribution of mean $\bar{n}_o + \bar{n}_s$ and standard deviation $[\bar{n}_o(1+2\bar{n}_s)]^{1/2}$, so that the theory of Jenkins and Watts (1968) should indeed apply. This theory is obviously preferable to the simple one, since it covers the whole spectrum and should be independent of signal strength.

4. Normalisation of the spectral estimators

In the previous section we have derived general expressions for the means and variances of the coefficients of the *unnormalised* autocorrelation function estimator and periodogram. Simulation for the autocorrelation function estimator revealed the effect of apparent misnormalisation between the simulated autocorrelation function and theory. As has been discussed (Oliver 1978), one can choose other possible means of normalisation which overcome this problem and give improved accuracy in the extraction of spectral parameters by fitting compared with the unnormalised situation. The three particular modes of normalisation which were applied in that paper to long data sets such that $N \gg k$, $N \to \infty$, were called true normalisation, self-normalisation and far-point normalisation. In this section we shall derive expressions for the mean and variance of each of these estimators for both the autocorrelation function and the periodogram. We shall assume a wide-band signal, as before, for simplicity. Specific comparison with simulation will be made for photodetection of a constant light source as before.

4.1. The autocorrelation function

4.1.1. Derivation of means and variances. As described in Oliver (1978), the normalised autocorrelation function $r(k)$ can be determined from the unnormalised one from the expression

$$r(k) = R(k)/\langle x\rangle^2. \tag{34}$$

However, in any real experiment one has only estimators for $R(k)$ and $\langle x\rangle$ denoted by $\hat{R}(k)$ and $\hat{x}$ respectively. Different combinations of estimators give rise to the differently normalised autocorrelation function estimators. The estimator for true normalisation, as in Oliver (1978), is represented by

$$\hat{r}_T(k) = \hat{R}(k)/\langle x\rangle^2 \tag{35}$$

where $\langle x\rangle$ is the average over many experiments, and $\hat{R}(k)$ is the estimate from a single experiment. Of course the denominator in equation (35) is not strictly speaking the mean value, but can approach it arbitrarily closely as the number of experiments is increased. In any case the discrepancy in this quantity can be reduced well below that in $\hat{R}(k)$. From equations (14), (16) and (17) we obtain

$$\langle \hat{r}_T(k)\rangle = R(k)/\langle x\rangle^2 = r(k) \tag{36}$$

and

$$\text{var } \hat{r}_T(k) = (N-k)^{-1}(\langle x^2\rangle^2/\langle x\rangle^4 - 1) \tag{37}$$

for $k \geqslant N/2$ with an additional term

$$+[2(N-2k)/(N-k)^2](\langle x^2\rangle/\langle x\rangle^4)\ \text{var } x$$

for $k \leqslant (N-1)/2$.

Suppose, however, we replace both $R(k)$ and $\langle x\rangle$ in equation (34) by the estimates obtained from a specific experiment so that

$$\hat{r}_S(k) = \frac{\hat{R}(k)}{\hat{x}^2} = \frac{1}{N-k}\sum_{j=0}^{N-1-k} x(j)x(j+k)\left(\frac{1}{N}\sum_{j=0}^{N-1} x(j)\right)^{-2} \tag{38}$$

where $\hat{r}_s(k)$ is the self-normalised autocorrelation function estimator. Expanding the numerator and denominator to first order about their mean values, as in Jakeman *et al* (1971b) and Oliver (1978), we obtain an expression for the bias given by

$$\langle \hat{r}_S(k)\rangle - r(k) \approx -(2/\langle x\rangle^3)(\langle \hat{R}(k)\,.\,\hat{x}\rangle - R(k)\langle x\rangle) + 3r(k)\ (\text{var } \hat{x})/\langle x\rangle^2 \tag{39}$$

with a variance given by

$$\text{var } \hat{r}_S(k) \approx (\text{var } \hat{R}(k))/\langle x\rangle^4 + 4r^2(k)[1 + (\text{var } \hat{x})/\langle x\rangle^2] - 4r(k)\langle \hat{R}(k)\,.\,\hat{x}\rangle/\langle x\rangle^3. \tag{40}$$

The unknown terms in equations (39) and (40) are next evaluated:

$$\text{var } \hat{x} = \langle \hat{x}^2\rangle - \langle \hat{x}\rangle^2 = \frac{1}{N^2}\sum_{j=0}^{N-1}\sum_{l=0}^{N-1}\langle x(j)x(l)\rangle - \left(\frac{1}{N}\sum_{j=0}^{N-1}\langle x(j)\rangle\right)^2$$

$$= \frac{\langle x^2\rangle}{N} - \langle x\rangle^2 + \sum_{j=0}^{N-1}\sum_{\substack{l\neq j\\ =0}}^{N-1}\langle x(j)x(l)\rangle. \tag{41}$$

For wide-band signals such that the last term factorises this reduces to

$$\text{var } \hat{x} = (\text{var } x)/N. \tag{42}$$

Similarly

$$\langle \hat{R}(k) \,.\, \hat{x} \rangle = \frac{1}{N(N-k)} \sum_{j=0}^{N-1} \sum_{l=0}^{N-1} \langle x(j)x(l)x(l+k) \rangle$$

$$= \frac{1}{N(N-k)} \left(2 \sum_{l=0}^{N-1-k} \langle x^2(l)x(l+k) \rangle + \sum_{l=0}^{N-1-k} \sum_{\substack{j \neq l \\ \neq l+k \\ =0}}^{N-1} < x(j)x(l)x(l+k) \rangle \right) \quad (43)$$

which, for wide-band signals, reduces to

$$\langle \hat{R}(k) \,.\, \hat{x} \rangle = \langle x \rangle^3 + 2\langle x \rangle (\text{var } x)/N. \quad (44)$$

Substitution from equations (41) and (43) into equations (39) and (40) will give general expressions for the bias and variance of the self-normalised estimator. In general this estimator may well be neither unbiased nor consistent. However, for wide-band signals the general expressions simplify to

$$\langle \hat{r}_S(k) \rangle - r(k) \approx -N^{-1} (\text{var } x)/\langle x \rangle^2 \quad (45)$$

for the bias and

$$\text{var } \hat{r}_S(k) \approx (N-k)^{-1} (\langle x^2 \rangle^2 / \langle x \rangle^4 - 1) - 4N^{-1} (\text{var } x)/\langle x \rangle^2 \quad (46)$$

for the variance when $k \geq N/2$. For $k \leq (N-1)/2$ an additional term

$$+[2(N-2k)/(N-k)^2](\text{var } x)/\langle x \rangle^2$$

must be included. In this case the self-normalised autocorrelation function estimator is both consistent and asymptotically unbiased. It is worth noting that, when $N \gg k$, $N \to \infty$, equation (46) reduces to the relevant long-data-set result of Oliver (1978).

The far-point normalisation technique can also be adopted, as shown in Oliver (1978), where the autocorrelation function decays to near its background value. The large delay value, $R(N-1)$, would then be approximately given by

$$R(N-1) \approx \langle x \rangle^2. \quad (47)$$

Thus we can define a far-point normalised correlation function by subtracting the estimator for the far point, i.e.

$$\hat{R}_F(k) = \hat{R}(k) - \hat{R}(N-1) \quad (48)$$

where $k < N-1$. Hence

$$< \hat{R}_F^2(k) \rangle = \langle \hat{R}^2(k) \rangle + \langle \hat{R}^2(N-1) \rangle - 2\langle \hat{R}(k) \,.\, \hat{R}(N-1) \rangle. \quad (49)$$

Expanding in terms of the original data and accounting for the special cases, the last term in equation (49) becomes

$$\langle \hat{R}(k) \,.\, \hat{R}(N-1) \rangle = \langle x \rangle^2 + \frac{2\langle x \rangle^2 \text{ var } x}{N-k} \quad (50)$$

for wide-band signals. Hence the variance of this estimator for wide-band signals can be shown to be given by

$$\text{var } \hat{R}_F(k) = \langle x^2 \rangle^2 - \langle x \rangle^4 + (\langle x^2 \rangle - 3\langle x \rangle^2)(\text{var } x)/(N-k) \quad (51)$$

when $k \geq N/2$. For $k \leq (N-1)/2$ an additional term

$$+[2(N-2k)/(N-k)^2]\langle x \rangle^2 \text{ var } x$$

should be included. Finally this estimator should be divided by the theoretical value of $R(N-1)(=\langle x\rangle^2)$ and the resultant added to 1 to make it consistent with the previous estimators, so that the complete far-point normalised autocorrelation function estimator is defined by

$$\hat{r}_F(k) = \hat{R}_F(k)/\langle x\rangle^2 + 1 = (\hat{R}(k) - \hat{R}(N-1))/\langle x\rangle^2 + 1. \tag{52}$$

This estimator has a mean value given by

$$\langle \hat{r}_F(k)\rangle = 1 + \langle \hat{R}(k)\rangle - \langle \hat{R}(N-1)\rangle)/\langle x\rangle^2. \tag{53}$$

For wide-band signals the mean becomes 1, since

$$\langle \hat{R}(k)\rangle = \langle \hat{R}(N-1)\rangle = \langle x\rangle^2.$$

Since both $\hat{R}(k)$ and $\hat{R}(N-1)$ are unbiased estimators, as shown by equation (14), the far-point normalised estimator is also unbiased. If we next consider the variance we obtain

$$\text{var } \hat{r}_F(k) = \langle x^2\rangle^2/\langle x\rangle^4 - 1 + [(\langle x^2\rangle - 3\langle x\rangle^2)/\langle x\rangle^4](\text{var } x)/(N-k) \tag{54}$$

when $k \geqslant N/2$. When $k \leqslant (N-1)/2$ an additional term

$$+[2(N-2k)/(N-k)^2](\text{var } x)/\langle x\rangle^2$$

should be included. From equation (54) it is apparent that this estimator is not consistent, since the variance is largely independent of N. This follows from the fact that the dominant term in the variance corresponds to the variance in $\hat{R}_F(N-1)$, which is always made up of only two data samples, $x(0)$ and $x(N-1)$, however large N.

For the sake of comparison with simulation we are going to consider photodetection of constant intensity. Substituting the relevant values of the moments for a Poisson distribution, $p(n)$, these variances become as follows:

$$\text{var } \hat{r}_T(k) = (N-k)^{-1}(1+2\bar{n})/\bar{n}^2 \tag{55}$$

when $k \geqslant N/2$ with an additional term

$$+[2(N-2k)/(N-k)^2](1+\bar{n})/\bar{n}^2$$

when $k \leqslant (N-1)/2$ for the estimator with true normalisation;

$$\text{var } \hat{r}_S(k) = (N-k)^{-1}(1+2\bar{n})/\bar{n}^2 - 4/N\bar{n} \tag{56}$$

when $k \geqslant N/2$ with an additional term

$$+[2(N-2k)/(N-k)^2](1/\bar{n})$$

when $k \leqslant (N-1)/2$ for the self-normalised estimator;

$$\text{var } \hat{r}_F(k) = (1+2\bar{n})/\bar{n}^2 + (N-k)^{-1}(1-2\bar{n})/\bar{n}^2 \tag{57}$$

when $k \geqslant N/2$ with an additional term

$$+[2(N-2k)/(N-k)^2](1/\bar{n})$$

when $k \leqslant (N-1)/2$ for the estimator with far-point normalisation.

4.1.2. Comparison of theory with simulation. As before, the comparison was made for the specific case of photodetection of a constant light intensity giving a mean count rate per sample time of $\bar{n} = 10$. The standard deviations of the different autocorrelation

function estimators were computed for 1000 batches of length $N = 128$ and are compared with theory in table 2; they show good agreement. Comparison of the standard deviations shows that self-normalisation is consistently the best method and far-point normalisation the worst. This latter finding differs from the equivalent one in Oliver (1978) because the error is dominated by that in the last delay, which is only made up of two samples in this case compared with approximately N for the long data set. From the point of view of the accuracy with which the autocorrelation coefficients can be determined, therefore, the self-normalised estimator is to be preferred.

Table 2. A comparison of the predicted standard deviations in the autocorrelation function estimator with the results of simulation over 1000 runs having $\bar{n} = 10$.

Normalization method	Delay (k)	Standard deviation	
		Simulation	Theory
True	1	0·058	0·057
	63	0·059	0·058
	127	0·45	0·46
Self	1	0·014	0·010
	63	0·017	0·014
	127	0·44	0·45
Far-point	1	0·45	0·46
	63	0·44	0·45
	126	0·33	0·34

4.2. The periodogram

4.2.1. Derivation of means and variances. When normalising the autocorrelation function, the calculated coefficients were divided by the value at very large delay, which is the same as that for finite delay with independent samples. The equivalent quantity in frequency space would be able to divide the spectral coefficients by that for very high frequency, which is the same as that at arbitrary frequency with a wide-band signal. From equation (24) we see that this coefficient is equal to var $x(\sigma_x^2)$. Thus, by analogy with the autocorrelation function, we can define a normalised periodogram by

$$p(\omega) = P(\omega)/\sigma_x^2. \tag{58}$$

Again, by analogy with the autocorrelation function treatment, we can define the periodogram with true normalisation by

$$\hat{p}_{\mathrm{T}}(\omega) = \hat{P}(\omega)/\langle\sigma_x^2\rangle \tag{59}$$

where $\langle\sigma_x^2\rangle$ is the ensemble average of the variance over many batches. For wide-band signals this normalised estimator will have the value 1, as shown by equation (24). The variance of this estimator is given by

$$\text{var } \hat{p}_{\mathrm{T}}(\omega) = 1 + (N\sigma_x^4)^{-1}(\langle x^4\rangle - 4\langle x\rangle\langle x^3\rangle - 3\langle x^2\rangle^2 + 12\langle x\rangle^2\langle x^2\rangle - 6\langle x\rangle^4) \tag{60}$$

for wide-band signals.

The self-normalised periodogram, on the other hand, could be defined as

$$\hat{p}_{\mathrm{S}}(\omega) = \hat{P}(\omega)/\hat{\sigma}_x^2 \tag{61}$$

where the periodogram estimator obtained during each batch is normalised by the estimate for the variance of x obtained in that batch. Performing a linear expansion of both numerator and denominator in equation (61) about their mean values, we obtain expressions for the bias and variance of this spectral estimator given by

$$\langle \hat{p}_S(\omega)\rangle - p(\omega) \approx p(\omega)\left(\frac{\langle(\hat{\sigma}_x^2)^2\rangle}{\sigma_x^4} - \frac{\langle \hat{P}(\omega)\,.\,\hat{\sigma}_x^2\rangle}{P(\omega)\sigma_x^2}\right) \tag{62}$$

and

$$\text{var}\,\hat{p}_S(\omega) \approx \frac{\text{var}\,\hat{P}(\omega)}{\sigma_x^4} - 2p(\omega)\frac{\langle \hat{P}(\omega)\,.\,\hat{\sigma}_x^2\rangle}{\sigma_x^4} + p^2(\omega)\left(1 + \frac{\langle(\hat{\sigma}_x^2)^2\rangle}{\sigma_x^4}\right). \tag{63}$$

The estimator for the variance of x can be defined by

$$\hat{\sigma}_x^2 = \widehat{x^2} - \hat{x}^2 \tag{64}$$

so that the unknown quantity $\langle(\hat{\sigma}_x^2)^2\rangle$ in equations (62) and (63) will be given by

$$\langle(\hat{\sigma}_x^2)^2\rangle = \langle(\widehat{x^2})^2\rangle - 2\langle \widehat{x^2}\,.\,\hat{x}^2\rangle + \langle \hat{x}^4\rangle \tag{65}$$

where

$$\langle(\widehat{x^2})^2\rangle = \frac{1}{N^2}\sum_{j=0}^{N-1}\sum_{k=0}^{N-1}\langle x^2(j)x^2(k)\rangle \tag{66}$$

$$\langle \widehat{x^2}\,.\,\hat{x}^2\rangle = \frac{1}{N^3}\sum_{j=0}^{N-1}\sum_{k=0}^{N-1}\sum_{l=0}^{N-1}\langle x^2(j)x(k)x(l)\rangle \tag{67}$$

and

$$\langle \hat{x}^4\rangle = \frac{1}{N^4}\sum_{j=0}^{N-1}\sum_{k=0}^{N-1}\sum_{l=0}^{N-1}\sum_{m=0}^{N-1}\langle x(j)x(k)x(l)x(m)\rangle. \tag{68}$$

Similarly

$$\langle \hat{P}(\omega)\,.\,\hat{\sigma}_x^2\rangle = \langle \hat{P}(\omega)\,.\,\widehat{x^2}\rangle - \langle \hat{P}(\omega)\,.\,\hat{x}^2\rangle \tag{69}$$

where

$$\langle \hat{P}(\omega)\,.\,\widehat{x^2}\rangle = \frac{1}{N^2}\sum_{j=0}^{N-1}\sum_{k=0}^{N-1}\sum_{l=0}^{N-1}\langle x^2(j)x(k)x(l)\rangle \exp[-i\Omega(k-l)] \tag{70}$$

and

$$\langle \hat{P}(\omega)\,.\,\hat{x}^2\rangle = \frac{1}{N^3}\sum_{j=0}^{N-1}\sum_{k=0}^{N-1}\sum_{l=0}^{N-1}\sum_{m=0}^{N-1}\langle x(j)x(k)x(l)x(m)\rangle \exp[-i\Omega(l-m)]. \tag{71}$$

Equations (65)–(71) can next be expanded in terms of diagonal and off-diagonal terms. In general the resultant expressions are very complicated, but for the case of wide-band signals such that the x's are uncorrelated, equations (65) and (69) simplify to

$$\langle(\hat{\sigma}_x^2)^2\rangle = \sigma_x^4 + N^{-1}(\langle x^4\rangle - 4\langle x\rangle\langle x^3\rangle - 3\langle x^2\rangle^2 + 12\langle x\rangle^2\langle x^2\rangle - 6\langle x\rangle^4) \tag{72}$$

and

$$\langle \hat{P}(\omega)\,.\,\hat{\sigma}_x^2\rangle = \sigma_x^4 + N^{-1}(\langle x^4\rangle - 4\langle x\rangle\langle x^3\rangle - 2\langle x^2\rangle^2 + 10\langle x\rangle^2\langle x^2\rangle - 5\langle x\rangle^4). \tag{73}$$

Substituting into equation (62) yields an expression

$$\langle \hat{p}_S(\omega)\rangle - p(\omega) \approx -1/N \tag{74}$$

for the bias of this estimator for wide-band signals, and an expression

$$\text{var } \hat{p}_S(\omega) \approx 1 - 2/N \tag{75}$$

for the variance. Both expressions are independent of the properties of x provided that it is a wide-band signal. From equation (74) we see that this estimator is biased to order $1/N$, i.e. asymptotically unbiased, while equation (75) shows that the estimator is still inconsistent. If the signal were narrow-band, so that the x's were correlated, then in general the self-normalised estimator would be both inconsistent and biased.

In order to calculate the effect of far-point normalisation we assume that the spectral coefficient at the maximum frequency should be given by σ_x^2 as already noted. As a first step, therefore, we define a far-point normalised estimator by

$$\hat{P}_F(\omega) = \hat{P}(\omega) - \hat{P}(\omega_m) \tag{76}$$

where ω_m (the highest-frequency component) $= 2\pi(N-1)/NT$. This estimator is unbiased since both $\hat{P}(\omega)$ and $\hat{P}(\omega_m)$ are unbiased as previously mentioned. The mean-square value of the estimator is given by

$$\langle \hat{P}_F^2(\omega)\rangle = \langle \hat{P}^2(\omega)\rangle - 2\langle \hat{P}(\omega)\,.\,\hat{P}(\omega_m)\rangle + \langle \hat{P}^2(\omega_m)\rangle \tag{77}$$

where

$$\langle \hat{P}(\omega)\,.\,\hat{P}(\omega_m)\rangle = \frac{1}{N^2}\sum_{j=0}^{N-1}\sum_{k=0}^{N-1}\sum_{l=0}^{N-1}\sum_{q=0}^{N-1}\langle x(j)x(k)x(l)x(q)\rangle \exp[-i\Omega(j-k)]$$
$$\times \exp[-i\Omega_m(l-q)] \tag{78}$$

Separating diagonal and off-diagonal terms, equation (78) can be reduced, for wide-band signals, to

$$\langle \hat{P}(\omega)\,.\,\hat{P}(\omega_m)\rangle = \sigma_x^4 + N^{-1}(\langle x^4\rangle - 4\langle x\rangle\langle x^3\rangle - 3\langle x^2\rangle^2 + 12\langle x\rangle^2\langle x^2\rangle - 6\langle x\rangle^4) \tag{79}$$

using the relationships

$$\sum_{k=0}^{N-1}\underbrace{\sum_{q\neq k}^{N-1}\sum_{\substack{j\neq q\\ \neq k}}^{N-1}}_{=0}\exp[-i\Omega(j-k)]\exp[-i\Omega_m(k-q)] = 2N$$

and

$$\sum_{j=0}^{N-1}\underbrace{\sum_{k\neq j}^{N-1}\sum_{\substack{l\neq k\\ \neq j}}^{N-1}\sum_{\substack{q\neq l\\ \neq k\\ \neq j}}^{N-1}}_{=0}\exp[-i\Omega(j-k)]\exp[-i\Omega_m(l-q)] = N^2 - 6N.$$

Combining equations (25) and (79) we obtain, for wide-band signals,

$$\text{var } \hat{P}_F(\omega) = 2\sigma_x^4. \tag{80}$$

In order to make this estimator compatible with the other two periodogram estimators we next normalise throughout by σ_x^2 and also add the theoretical value at ω_m. Thus

$$\hat{P}_F(\omega) = (\hat{P}(\omega) - \hat{P}(\omega_m) + P(\omega_m))/\sigma_x^2. \tag{81}$$

For wide-band signals this is equal to 1. Under the same conditions the variance, from equation (80), is equal to 2, which means that this also is an inconsistent estimator.

As noted in § 3.1.1 the value of the periodogram away from the peak with narrow-band signals is not equal to σ_x^2. However, if the definitions of the estimators for the different normalisations are applied as given here during simulation, then a comparison of the variances should be consistent with the theoretical results given here. For initial comparison with simulation we use again photodetection of constant intensity light, in which case the variances of the three estimators are as follows:

$$\text{var } \hat{p}_T(\omega) = 1 + 1/N\bar{n} \tag{82}$$

for true normalisation;

$$\text{var } \hat{p}_S(\omega) \approx 1 - 2/N \tag{83}$$

for self-normalisation; and

$$\text{var } \hat{p}_F(\omega) = 2 \tag{84}$$

for far-point normalisation.

4.2.2. Comparison of theory with simulation. The simulation for light of constant intensity, $\bar{n} = 10$, was performed on the identical data to those used in the equivalent comparison for the autocorrelation function estimators. The results are summarised in table 3. Since the variance of the periodogram is not expected to depend on frequency for wide-band signals, the variance is averaged over all the coefficients except zero frequency. Firstly, it is apparent that the agreement between simulation and theory is within experimental error, demonstrating that the process has been truly represented by the theory. Secondly, it is shown that, as with the autocorrelation function, the self-normalised periodogram has the smallest statistical fluctuations in the coefficients, while far-point normalisation has the largest.

Table 3. A comparison of the predicted standard deviations in the periodogram estimator with the results of simulation over 1000 runs having $\bar{n} = 10$.

Normalization method	Standard deviation	
	Simulation	Theory
True	1·001 ± ·006	1·004
Self	0·982 ± ·010	0·984
Far-point	1·40 ± 0·01	1·41

4.3. Summary of spectral estimator properties

A summary of the properties of the different spectral estimators considered in this section is presented in table 4. This is based on the assumption that we have wide-band signals. For each normalisation technique we give an order of merit (in terms of the standard deviation of the estimator coefficients), the bias and the consistency of the estimator. We can conclude that, provided a bias of order $1/N$ is not an over-riding limitation, it is advantageous to use the self-normalised estimator in either time-delay

Table 4. A comparison of the properties of the differently normalised spectral estimators.

Estimator	Order of merit	Normalization method	Bias	Consistency
Autocorrelation function	2	True	None	Consistent
	1	Self	Order $(1/N)$	Consistent
	3	Far-point	Order $(1/N)$	Inconsistent
Periodogram	2	True	None	Inconsistent
	1	Self	Order $(1/N)$	Inconsistent
	3	Far-point	None	Inconsistent

or frequency space. If this bias is a limitation, then true normalisation (or no normalisation) should be adopted. In no situation does far-point normalisation have an advantage.

Since the comparison of table 4 has been applied for the case of wide-band signals, we shall conclude the section by a comparison of simulation with theory for heterodyne photodetection of narrow-band Gaussian–Lorentzian light. Simulation was performed for 3200 batches with each type of normalisation and both spectral estimators. The simulation parameters were: batch length $N = 128$, $\bar{n}_o = 10$, $\bar{n}_s = 1$, coherence time = 10 sample times, period = 10 sample times.

Since this simulation is no longer in the weak-signal limit, the approximate theory for the variances of the spectral estimators will no longer apply. We can make a meaningful comparison, therefore, solely in terms of the mean values of the estimators. The unnormalised forms of these were given in equations (31) and (33) for the autocorrelation function and periodogram respectively. On normalising these estimators we divide them by $\langle x \rangle^2$ and σ_x^2 respectively, as shown in equations (34) and (58). The value of the former is independent of the signal properties, being given by

$$\langle x \rangle^2 = (\bar{n}_o + \bar{n}_s)^2. \tag{85}$$

The latter depends on the signal properties. In the present case we have narrow-band Gaussian–Lorentzian light so that

$$\sigma_x^2 = \bar{n}_o(1 + 2\bar{n}_s) + \bar{n}_s(1 + \bar{n}_s) \tag{86}$$

(Jakeman and Pike 1969). The theoretical forms of the two estimators are then

$$r(k) = 1 + \frac{2\bar{n}_o\bar{n}_s}{(\bar{n}_o + \bar{n}_s)^2}\cos(\omega_0 kT)\exp(-|\Gamma kT|) + \frac{\bar{n}_s^2}{(\bar{n}_o + \bar{n}_s)^2}\exp(-|2\Gamma kT|) + \frac{\delta_{k,0}}{\bar{n}_o + \bar{n}_s} \tag{87}$$

for the autocorrelation function and

$$\begin{aligned} p(\omega) = 1 &+ \frac{2\bar{n}_o\bar{n}_s e^{-\gamma}}{\bar{n}_o(1 + 2\bar{n}_s) + \bar{n}_s(1 + \bar{n}_s)}\left(\frac{\cos\Omega_s - e^{-\gamma}}{1 - 2e^{-\gamma}\cos\Omega_s + e^{-2\gamma}} + \frac{\cos\Omega_d - e^{-\gamma}}{1 - 2e^{-\gamma}\cos\Omega_d + e^{-2\gamma}}\right) \\ &+ \frac{2\bar{n}_s e^{-2\gamma}}{\bar{n}_o(1 + 2\bar{n}_s) + \bar{n}_s(1 + \bar{n}_s)}\frac{\cos\Omega - e^{-2\gamma}}{1 - 2e^{-2\gamma}\cos\Omega + e^{-4\gamma}} \\ &+ \frac{N\delta(\omega)(\bar{n}_o + \bar{n}_s)^2}{\bar{n}_o(1 + 2\bar{n}_s) + \bar{n}_s(1 + \bar{n}_\sigma)} \end{aligned} \tag{88}$$

for the periodogram. The different normalisation methods have already been described. For true normalisation the individual estimators, defined in equations (35) and (59), are divided by the theoretical values of $\langle x \rangle^2$ and σ_x^2, given in equations (85) and (86) respectively, as appropriate. For self-normalisation, defined in equations (38) and (61), the estimators are divided by the individual estimators $\hat{x}^2$ and $\hat{\sigma}_x^2$ as appropriate. For far-point normalisation, defined in equations (52) and (81), the last channel of the spectral estimator is subtracted from the others, and the theoretical values of this channel added, before dividing throughout by the appropriate theoretical normalisation factor, $\langle x \rangle^2$ or σ_x^2.

The comparison of the theoretical and simulated autocorrelation functions in figure 3(*a*) shows that the averaged true and self-normalised estimators are effectively identical and are virtually indistinguishable from the theoretical values. The far-point normalised function is significantly different due to the error in the far-point coefficients. One would expect this misnormalisation compared with the theory to lead to poor statistical accuracy in the determination of spectral parameters by least-squares fitting to this estimator. Since this error corresponds to uncertainty in the total counts per batch, one would expect it to be reflected only in the zero-frequency component of the periodogram. The comparison of theory and simulation for the periodogram in figure 3(*b*) confirms this, showing that for non-zero frequencies all the estimators are very close to the theoretical values. A slight departure of the self-normalised data from theory over the peak is observable, but the estimators with true and far-point normalisation are indistinguishable. One might expect, therefore, that fitting the periodogram should yield the same statistical accuracy with each normalisation technique.

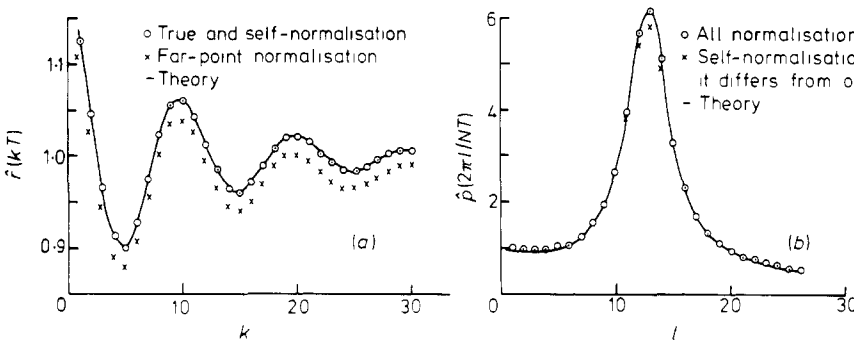

Figure 3. A comparison of the different normalisation techniques for (*a*) the autocorrelation function estimator and (*b*) the periodogram. The results are for heterodyne photodetection of narrow-band Gaussian–Lorentzian light under the following conditions: 3200 batches, $N = 128$, $\bar{n}_o = 10$, $\bar{n}_s = 1$, $\tau_c/T = 10$, $\tau_p/T = 10$. The full curves represent theory.

5. Relative accuracy in the extraction of spectral parameters by fitting

So far the analysis has been restricted to a discussion of the relative errors in the coefficients of the different estimators. A sometimes more useful comparison would be couched in terms of the accuracy with which spectral parameters can be determined from each of the estimators. In particular we wish to establish: (i) whether one achieves greater accuracy using the periodogram or the autocorrelation function estimator; (ii)

which normalisation technique gives the best accuracy in each case. The discussion in § 3 established the analytic equivalence of the unnormalised periodogram and autocorrelation function estimators, which suggests that the two methods should give equivalent accuracy, modified only by the different weightings given to the parameters when fitting in their frequency or time space. In Oliver (1978) it was demonstrated that for heterodyne detection each normalisation technique, using autocorrelation functions from long data batches, gave the same accuracy. However, in the previous section we have shown that the variance of the far-point estimator for the correlation function is much greater than the others, which one would expect to change the previous conclusion.

The various normalisation techniques for the two spectral estimators were therefore compared by simulation followed by fitting to the analytic forms given in equations (31) and (33) above. The statistical accuracy in a single run was not adequate for fitting, so a series of 16 independent batches were simulated; the normalised spectral estimators were calculated and the results averaged and then fitted. The parameters used in the simulation were: 200 sets of 16 batches of length $N = 128$ samples, $\bar{n}_o = 10$, $\bar{n}_s = 1$, coherence time $\tau_c = 10$ sample times, period $\tau_p = 10$ sample times. The results are summarised in table 5.

Table 5. The mean values and standard deviations of the spectral parameters for coherence time (τ_c) and period (τ_p) for the two spectral estimators and the different normalisation methods.

Spectral estimator	Normalization method	τ_c	$\Delta\tau_c$	τ_p	$\Delta\tau_p$
Correlation function	True	10·4	1·9	9·99	0·22
	Self	10·4	2·1	9·99	0·21
	Far-point	10·5	7·1	9·96	0·23
Periodogram	True	10·6	2·3	10·00	0·24
	Self	10·2	2·2	10·00	0·24
	Far-point	10·6	2·5	10·01	0·25

Within experimental error the standard deviations in the estimated period $\hat{\tau}_p$ are the same. However the standard deviation in the coherence time $\hat{\tau}_c$ determined from the far-point normalised autocorrelation function is significantly greater than the rest, which appear similar to each other. With this exception, therefore, all the possibilities yield the same statistical accuracy in the spectral parameters. From this point, therefore, we shall only consider the self-normalised spectral estimators as representing the five best methods. While this choice is not significant for heterodyne detection, it has already been demonstrated (Oliver 1978) that this is the best autocorrelation function estimator to be used in either direct or homodyne detection.

6. Long data sets

As we have already shown, the periodogram is an inconsistent spectral estimator. Thus if we wish to achieve a resolution of 1 part in N, the data batch should be of length N. If one has long data sets of $M(\gg N)$ samples, one can achieve improved accuracy with the

same resolution by various methods which are basically equivalent to averaging over M/N independent batches each of length N. With the autocorrelation function, however, the estimator can be constructed for N delays but with M samples in the usual manner as analysed in Oliver (1978). It is obviously important to establish whether there are any significant differences in the accuracy that can be achieved in the determination of the spectral parameters depending on whether one uses a single long data set (length M) and merely calculates N delay coefficients, or averages over M/N independent autocorrelation function estimators from batches of length N.

If we consider first the autocorrelation function estimators, then, averaging over M/N independent batches, the variance of the estimator can be shown from equation (46) to be given by

$$\text{var } \hat{r}_S(k) = [N/M(N-k)](\langle x^2\rangle^2/\langle x\rangle^4 - 1) - 4(\text{var } x)/M\langle x\rangle^2 \tag{89}$$

for $k \geqslant N/2$ with an additional term

$$+[2N(N-2k)/M(N-k)^2](\text{var } x)/\langle x\rangle^2$$

for $k \leqslant (N-1)/2$. The equivalent result for the long data set was given in Oliver (1978) as

$$\text{var } \hat{r}_S(k) = M^{-1}\left(\frac{\langle x^2\rangle^2}{\langle x\rangle^4} - 1\right) - 2(\text{var } x)/M\langle x\rangle^2. \tag{90}$$

This is identical to equation (89) when $N \gg k$. For heterodyne detection in the weak-signal limit, equation (89) yields

$$\text{var } \hat{r}_S(k) \approx [N/M(N-k)](2\bar{n}_o + 1)/\bar{n}_o^2 - 4/M\bar{n}_o \tag{91}$$

for $k \geqslant N/2$ with an additional term

$$+[2N(N-2k)/M(N-k)^2](1/\bar{n}_o)$$

for $k \leqslant (N-1)/2$. Similarly the single long data set would give

$$\text{var } \hat{r}_S(k) \approx M^{-1}(2\bar{n}_o + 1)/\bar{n}_o^2 - 2/M\bar{n}_o. \tag{92}$$

For the periodogram, averaging over M/N batches of wide-band signals would be expected to give a variance a factor M/N smaller, so that, from equation (75), we obtain

$$\text{var } \hat{r}_S(\omega) = N/M - 2/M. \tag{93}$$

However, for arbitrary signals it has been shown (equation (26)) that the variance is best represented by the square of the spectrum. Thus the variance of the self-normalised periodogram would be expected to be given by

$$\text{var } \hat{p}_S(\omega) \approx (N/M)(p(\omega))^2 \tag{94}$$

where $p(\omega)$ is the exact normalised spectrum for the truncated batch.

The theoretical predictions of equations (91), (92) and (94) are compared with simulation under the same conditions as applied in table 5, and the results are given in table 6. The agreement between simulation and theory for the periodogram is close, showing that the error is dominated by that in the periodogram with true normalisation. This is to be expected, since the correction on self-normalisation is of order $1/N$ smaller than the first term derived for the unnormalised periodogram. The agreement between theory and simulation for the autocorrelation function estimators is worse than that demonstrated in figure 1, resulting from the high value of $\bar{n}_s$ (=1) used for the present

Table 6. A comparison of the theoretical and simulated standard deviations for the periodogram and autocorrelation function estimator coefficients. The effects of averaging over short batches and taking long data sets are included.

Periodogram $\hat{p}_S$ $(2\pi l/NT)$			Autocorrelation function $\hat{r}_S(kT)$				
l	Averaged batches		k	Averaged batches		Long data set	
	Theory	Simulation		Theory	Simulation	Theory	Simulation
1	0·25	0·23	1	0·006	0·011	0·015	0·034
13	1·46	1·23	63	0·009	0·012	0·015	0·026
63	0·097	0·101	127	0·19	0·18	0·015	0·028

simulation. This leads to much greater correlation between neighbouring samples than in the weak-signal case, which in turn results in a discrepancy between the simple model and a full theory. If we consider the theoretical predictions for the standard deviation of the self-normalised autocorrelation function, which would be applicable only in the weak-signal limit, then it is apparent that using the long data set gives slightly better accuracy. Where signal statistics dominate, the simulation comparison demonstrates that greater accuracy is achieved by averaging over many short batches for values of k less than 90 than by using the long data set. One might therefore expect an advantage to accrue from using the former technique when extracting the value of spectral parameters by fitting procedures in this situation.

The most significant comparison between a long data set and the average over many short batches lies in the accuracy with which spectral parameters can be obtained in a given situation. In order to make such a comparison, therefore, we again adopt simulation of heterodyne photodetection of Gaussian–Lorentzian light. With the exception of the coherence time, the conditions are identical to those in tables 5 and 6; i.e. a total of 2048 samples either in one set or in batches of 128, $\bar{n}_o = 10$, $\bar{n}_s = 1$, and period = 10 sample times. The ratio of the coherence time to the sample time (τ_c/T) is then varied over values of 5, 10, 20, 40, 80 and 160; the periodogram and autocorrelation function averaged over 16 batches of length 128 and the autocorrelation function containing 128 delays made up of 2048 samples are constructed, and each spectral estimator fitted to the relevant theoretical form. The results are illustrated in figure 4. While it is difficult to draw any hard and fast conclusions, it is apparent that averaging over short batches offers an improvement of about 40% compared with the long data set for both period and coherence time under the conditions chosen. However, in all cases the mean values of the coherence time determined by fitting when the coherence time is comparable with the number of delay coefficients (128) in the autocorrelation function are significantly reduced compared with the input parameters. It appears that if one has a data batch of length N, or N autocorrelation coefficients for a long data set, then the coherence time will be underestimated if it exceeds about $NT/2$. Apart from this limitation, each method shows a similar dependence of the accuracy on the coherence time. Over the range $5 \leqslant \tau_c/T \leqslant 40$ the results for the long-data-set autocorrelation function are in good agreement with those in the previous paper (Oliver 1978). Many of the conclusions of that paper regarding choice of operating conditions can be expected to apply when short data batches are averaged as well as when long data sets are taken, since the dependence on coherence time is similar.

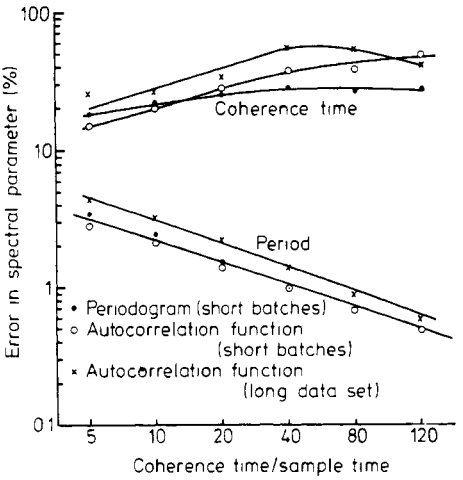

Figure 4. A comparison of the accuracy in linewidth and period obtained for different estimators under the same conditions as in figure 3, except that the coherence time is varied.

7. Conclusions

The equivalence of the periodogram and autocorrelation function estimator for short batches of data has been demonstrated both theoretically and by computer simulation followed by fitting to determine spectral parameters. There is therefore no theoretical advantage to be gained when processing batch data from operating in either frequency or time domains. Such advantages that do occur will result from an engineering comparison of the departures from exact operation in either domain, e.g. the question of linearity or many-bit operation.

Secondly, it has been shown that there is no significant advantage either from consideration of distortion or statistical accuracy in using long data sets compared with averaging over several short batches of data. Indeed the latter method seems to offer a slight advantage where strong signals are encountered. Thus a batch-processing Fourier transform would offer advantages over a continuous autocorrelation function method (~40%) which may compensate for possibly reduced efficiency of such a system unless it is multiplexed.

Thus any comparison between implementations in the two domains must be in terms of engineering constraints and limitations.

References

Brillinger D R and Rosenblatt M 1967 in *Spectral Analysis of Time Series* ed. B Harris (New York: Wiley).
Butler M B N 1977 *Agard Conference Preprint No.* 230
Degiorgio V and Lastovka J B 1971 *Phys. Rev.* A **4** 2033
Foord R, Jakeman E, Jones R, Oliver C J and Pike E R 1969 *IERE Conf. Proc. No. 14*
Foord R, Jakeman E, Oliver C J, Pike E R, Blagrove R J, Wood E and Peacocke A R 1970 *Nature* **227** 242
Hannan E J 1960 *Time Series Analysis* (London: Methuen)
Hughes A J, Jakeman E, Oliver C J and Pike E R 1973 *J. Phys. A: Math., Nucl. Gen.* **6** 1327
Jakeman E 1972 *J. Phys. A: Gen. Phys.* **5** L49
—— 1974 in *Photon-correlation and Light-beating Spectroscopy* ed. H Z Cummins and E R Pike (New York: Plenum) p 75

Jakeman E and Pike E R 1969 *J. Phys. A: Gen. Phys.* **2** 115
Jakeman E, Oliver C J and Pike E R 1971a *Phys. Lett.* A **34** 101
Jakeman E, Pike E R and Swain S 1970 *J. Phys. A: Math. Gen.* **3** 255
—— 1971b *J. Phys. A: Math. Gen.* **4** 517
Jenkins G M and Watts D G 1968 *Spectral Analysis and its Applications* (San Francisco: Holden-Day)
Kelly H C 1971 *J. Quant. Electron. (IEEE)* **7** 541
Koppel D E 1974 *Phys. Rev.* A **10** 1938
Mandel L 1959 *Proc. Phys. Soc.* **74** 233
Oliver C J 1974 in *Photon-correlation and Light-beating Spectroscopy* ed. H Z Cummins and E R Pike (New York: Plenum) p 151
—— 1978 *Adv. Phys.* **27** 387–436
Oppenheim A V and Schafer R W 1975 *Digital Signal Processing* (New Jersey: Prentice-Hall)
Pike E R 1977 in *Photon-correlation and Velocimetry* ed. H Z Cummins and E R Pike (New York: Plenum) p 246
Saleh B E A and Cardoso M F 1973 *J. Phys. A: Gen. Phys.* **6** 1897